Antifouling bastadin congeners target blue mussel phenoloxidase and complex copper(II) ions

Journal:	*Marine Biotechnology*
Manuscript ID:	Draft
Manuscript Type:	Original Article
Date Submitted by the Author:	n/a
Complete List of Authors:	Bayer, Mirko; Heinrich-Heine-Universität Düsseldorf, Institut für Pharmazeutische Biologie Hellio, Claire; Portsmouth University, School of Biological Sciences Marechal, Jean-Philippe; Portsmouth University, School of Biological Sciences Lin, Wenhan; Peking University, State Key Laboratory of Natural and Biomimetic Drugs Frank, Walter; Heinrich-Heine-Universität Düsseldorf, Institut für Anorganische Chemie und Strukturchemie Weber, Horst; Heinrich-Heine-Universität Düsseldorf, Institut für Pharmazeutische und Medizinische Chemie Proksch, Peter; Heinrich-Heine-Universität Düsseldorf, Institut für Pharmazeutische Biologie
Keywords:	Mytilus edulis, mussel phenoloxidase, antifouling, bastadins, hemibastadin, dibromohemibastadin

Antifouling bastadin congeners target blue mussel phenoloxidase and complex copper(II) ions

Mirko Bayer[1,6], Claire Hellio[3], Jean-Philippe Marechal[3], Wenhan Lin[5], Walter Frank[4], Horst Weber[2], Peter Proksch[1a]

[1]Institut für Pharmazeutische Biologie und Biotechnologie, Heinrich-Heine-Universität Düsseldorf, Universitätsstr. 1, 40225 Düsseldorf, Germany

[2]Institut für Pharmazeutische und Medizinische Chemie, Heinrich-Heine-Universität Düsseldorf, Universitätsstr. 1, 40225 Düsseldorf, Germany

[3]School of Biological Sciences, King Henry Building, Portsmouth University, Portsmouth PO1 2DY, United Kingdom

[4]Institut für Anorganische Chemie und Strukturchemie, Heinrich-Heine-Universität Düsseldorf, Universitätsstr. 1, 40225 Düsseldorf, Germany

[5]State Key Laboratory of Natural and Biomimetic Drugs, Peking University, PR China

[6]Caesar & Loretz GmbH, Herderstr. 31, 40721 Hilden, Germany

[a]corresponding author: Prof. Dr. Peter Proksch, proksch@uni-duesseldorf.de, 0049-211-81-14170

Abstract

Synthetically prepared congeners of sponge-derived bastadin derivatives such as DBHB that suppress the settling of barnacle larvae were identified in this study as strong inhibitors of blue mussel phenoloxidase that is involved in firm attachment of mussels and of other marine fouling organisms to a given substrate. The IC_{50} value of DBHB as the most active enzyme inhibitor encountered in this study amounts to 0.84 µM. Inhibition of phenoloxidase by DBHB is likely due to complexation of copper(II) ions from the catalytic centre of the enzyme by the α-oxo-oxime moiety of the compound as shown here for the first time by structure activity studies and by X-ray structure determination of a copper(II) complex of DBHB.

Abbreviations: 2,3-BMO (2,3-butanedione monoxime), DBHB (6,6'-dibromo-hemibastandin-1), DMF (dimethylformamide), NBHB (norbromohemibastadin-1), TBT (tri-n-butyl tin oxide), TT (tyrosinyltyramine)

Keywords: *Mytilus edulis*, mussel phenoloxidase, antifouling, bastadins, hemibastadin, dibromohemibastadin, norbromohemibastadin, tyrosinyltyramine, 2,3-butanedione monoxim, x-ray, copper(II), copper complex, natural products

Introduction

Man-made as well as natural surfaces in the marine ecosystem are rapidly colonized by fouling organisms that include microorganisms, algae, barnacles, mussels and others. Biofouling causes significant economical wastage worldwide e.g. by reducing boat speeds and increasing fuel consumption (Wahl 1989, Yebra et al. 2004). Considering that up to 90% of global trade rely on ships serious problems due to biofouling arise for the maritime industry (Liu et al. 1997, Voulvoulis et al. 1999, Marechal and Hellio 2009). Until recently, coatings containing tri-*n*-butyl tin oxide (TBT) were used for preventing biofouling. Since 2008 usage of TBT is banned by the International Maritime Organisation (IMO 2001, Voulvoulis et al. 1999, Lau 1991, Pereira and Ankjaergaard 2009) and new antifouling strategies, involving chemical, physical, and mechanical mechanisms, are urgently needed to replace TBT and other potentially toxic or harmful ingredients (Hellio and Yebra 2009).

The frequently made observation that many sponges are conspicuously free of overgrowth caused by fouling organisms has stimulated the search for naturally occurring antifouling leads from marine sponges (e.g. Tsoukatou et al 2002, Fusetani 2004, Tsoukatou et al 2007, Hellio et al 2009). In this context we demonstrated recently significant antifouling activity for sponge-derived bastadin and hemibastadin derivatives and for several synthetically derived analogues such as DBHB using larvae of the barnacle *Amphibalanus* improvisus (Darwin, 1854) as a model organism (Ortlepp et al., 2007). Bastadins are tyrosine-derived, brominated, oxime bearing peptides that can be cyclic or linear and are typical constituents of marine sponges from the genus *Ianthella* such as *I. basta* (Ortlepp et al. 2007). Hemibastadin-1 is the simplest bastadin derivative known and can be considered as a biogenetic precursor of the larger bastadins including two or more hemibastadin moieties that are usually

linked through ether functions. Hemibastadin-1 as well as its closely related synthetically derived analogue DBHB suppresse settling of barnacle larvae at low micromolar concentrations making these compounds interesting candidates in the search for new antifouling constituents from nature especially as they are easily accessible by organic synthesis (Ortlepp et al. 2007).

It is well known that phenoloxidases of mussels and of other marine invertebrates such as barnacle larvae are highly relevant for settling of these fouling organisms since they are involved in polymerization of secreted proteins called foot proteins (Aladaileh et al. 2007, Hellio et al. 2000, Zentz et al. 2001). The latter contain numerous residues of the aromatic amino acids phenylalanine and tyrosine. Phenoloxidases oxidize these aromatic amino acids and form highly reactive ortho-di-quinone bearing systems that cross-react with each other as well as with other proteins and generate a biopolymer, which firmly attaches the fouling organism to a suitable surface (Suci and Geesey 2000, Aladaileh et al. 2007, Kamino 2001, Cheung et al. 1977). In order to prevent a spontaneous polymerization of aromatic amino acids phenoloxidase is stored intracellularly as enzymatically inactive pro-phenoloxidase. Chemical transformation and activation of pro-phenoloxidase to phenoloxidase is proteolytically catalyzed during secretion by different proteases that are controlled by Ca^{2+} dependant signalling cascades (Asokan et al. 1997, Hellio et al. 2007). It is known that intracellular Ca^{2+} concentration is important for settling (Rittschof et al. 1986, Clare 1996, Yamamoto et al. 1999). Thus, by reduction of Ca^{2+} influx the signalling cascades that are involved in proteolytic conversion of pro-phenoloxidase and in secretion of the active phenoloxidase can be inhibited. TBT interferes with the cellular calcium regulator calmodulin and thus reduces mussel

phenoloxidase activity (Cima and Ballarin 2000, Cima et al. 1998a,b, Tujula et al. 2001).

A further strategy for inhibiting the attachment of fouling organisms is the search for direct enzyme inhibitors of phenoloxidase. This family of oxygen activating enzymes is distinguished by containing copper(II) ions that are bound to histidin moieties in the catalytic centre playing an essential role for the activity of these enzymes (Kim and Uyama 2005; Olivares et al. 2002). If a suitable phenolic substrate draws close to the active site of the enzyme, hydroxylation and further oxidation is performed by electron transfer from copper via oxygen to the substrate (Decker et al. 2000). Complexation of copper ions would thus be a powerful way of inhibiting the enzymatic activity of phenoloxidase and as a result attachment of fouling organisms.

Several inhibitors of phenoloxidases are already known from natural sources, like quercetin and other flavonoids, mimosine or kojic acid (Kubo et al. 2000, Chen et al. 1991, Kim and Uyama 2005, Kim et al. 2006). Some synthetically derived halogenated phenols have also been reported to inhibit phenoloxidases (Nagasawa et al. 1981). Hemibastadin, however, has so far not been investigated as an inhibitor of marine-derived phenoloxidases. In this study we explore the mode of action of hemibastadins and of related compounds with regard to their antifouling activity and report on:

- Inhibition of purified blue mussel phenoloxidase by DBHB and by some of its derivatives *in vitro*
- Ability of these compounds to complex copper(II) ions
- X-ray analysis of a distinct complex of DBHB with copper(II) chloride, crystallized from DMF and dichloromethane

Results

Several synthetically prepared hemibastadin-1 congeners that included DBHB, NBHB, and TT that differs from the former two compounds by absence of bromine atoms in the aromatic rings and by replacement of the oxime function of the hemibastadin-congeners by an amine substituent were selected for *in vitro* studies with phenoloxidase prepared from the blue mussel *Mytilus edulis*. 2,3-Butanedione monoxime (2,3-BMO) that is likewise of synthetic origin was also included in the experiments as it features an α-oxo-oxime moiety and thus resembles an important characteristic functionality of DBHB and NBHB but lacks the aromatic rings of the latter two compounds. Nearly all compounds analyzed proved to be inhibitors of mussel phenoloxidase albeit at very different concentrations. DBHB was by far the strongest inhibitor encountered with an IC_{50} value of 0.84 µM. Next in activity was NBHB with an IC_{50} of 2.41 µM followed by 2,3-BMO with an IC_{50} value of 8.70 µM thereby indicating a clear enhancing effect of the phenolic rings and of the bromine substituents on the enzyme inhibitory activity of the compounds. TT, if at all, was by far the weakest inhibitor detected in this study, its IC_{50} value was > 83 µM (**Fig. 1**). This latter finding underlines the striking importance of the α-oxo-oxime function for inhibition of mussel phenoloxidase especially when viewed in comparison with the data achieved for the structurally closely related NBHB.

Complexation of free copper(II) ions by DBHB was determined photometrically in methanolic solution. Addition of increasing amounts of copper(II) sulphate to an arbitrarily chosen concentration of DBHB resulted in the formation of a distinct bathochromic band (green colour) at 685 nm in the VIS absorption spectrum (**Fig. 2**). Absorption intensity was found to increase upon addition of further amounts copper(II) sulphate. Maximum absorption was reached after a five to tenfold molar excess of

the copper salt in relation to DBHB (**Fig. 3**). NBHB and 2,3-BMO were likewise able to complex copper(II) ions as shown by the green coloration of a methanolic solution of the compounds following addition of copper(II) sulphate (data not shown) whereas no effect was observed for TT.

Subsequently we were able to prepare a neutral complex of DBHB with Cu(II) ions. When a solution of DBHB in methanol is mixed with an aqueous copper(II) acetate solution and the pH is adjusted to >9 by addition of sodium acetate, a brown precipitate is formed that can be separated. After drying a cocoa like powder remains that is insoluble in all common solvents but readily soluble in dilute HCl under decolourization and precipitation of DBHB. Addition of dilute NaOH forms a clear deep green coloured solution. Chemical composition of the brown powder was determined by elementary analysis showing that one copper(II) ion is bound to two molecules of DBHB (**Fig. 4**). Whereas this amorphous material was unsuitable for X-ray analysis, we were successful in preparing a macrocystallinic complex of DBHB with copper(II) chloride, which was crystallized from DMF and dichloromethane.

In parallel the crystal structure of free DBHB was likewise analyzed by X-ray analysis. Both crystal structures are reported here for the first time. Crystal data and details of the structure determination processes are presented in the materials and methods section. Representative geometrical data for both structures are summarized in **Tab. 1** and **Tab. 2**. These data in combination with **Fig. 5** allow for a detailed analysis of copper coordination and of the ligand properties of DBHB. The metal centres of the centrosymmetric dinuclear complex exhibit the typical 4+2-coordination mode of a Jahn-Teller distorted octahedral complex with a terminal (Cl2) and a bridging (Cl1a) chloride ligand occupying the axial positions. As to be expected the corresponding

Cu-Cl bond lengths are much larger than the length of the equatorial Cu1-Cl1 bond. According to the observed Cu-O and Cu-N distances strong bonding between the copper centre and the chelating DBHB ligand as well as the DMF ligand has to be assumed. Comparison of the relevant geometrical parameters of free and complexed DBHB (right half of **Tab. 1**) gives evidence for the high complexation potential of DBHB towards copper(II) ions. From the coordination chemistry point of view dinuclear copper complexes with a $Cu_2(\mu\text{-}Cl)_2$ core and a μ-Cl,Cl_2,O_2,N-coordination motif are very rare species (Kapoor et al. 2002, Kapoor et al. 2004) and we here present the first example of such a complex containing chlorido ligands in both the axial positions of the distorted hexacoordinated copper centers. In principle the closest structural relationship is given to di-μ-chloridobis((N,N''-2-pyrdyl-2'-pyridinium ketone oxime)aquachlorido-copper(II)) (Sommerer et al. 1995), a $Cu_2(\mu\text{-}Cl)_2$ core-complex with copper centers that are hexacoordinated in a μ-Cl, Cl_2,N2,O-mode with a μ-Cl and an aqua ligand in axial positions and the N,N'-chelating pyridyl ketone oxime ligand as well as two Cl ligands in equatorial postions. Comparison of the relevant bond lengths gives further evidence that bonding of DBHB to copper centers is comparatively strong. As can be seen from **Fig. 5** and the hydrogen bond parameters listed in **Tab. 2**, DBHB bonded to the copper centers is further involved in supramolecular interactions. It has to be assumed that its H bridging donor and acceptor properties also play an important role in the receptor binding process.

Complexation of copper(II) ions is not restricted to DBHB or other synthetic congeners such as NBHB or 2,3-BMO but extends also to naturally occurring bastadin derivatives that share the same important structural elements (α-oxo-oxime group) as shown by treatment of a crude aqueous methanolic extract of the sponge *I. basta* with an excess of copper(II) sulphate. A brown precipitate was formed after

addition of sodium carbonate solution which was separated and disintegrated with dilute HCl. The acidic solution was extracted with ethyl acetate followed by HPLC and LC-MS analysis. It revealed an enriched complex mixture of several known bastadin derivatives (data not shown) that had been formerly described from the same sponge (Ortlepp et al., 2007) thereby indicating that also naturally occurring bastadins have the capacity to complex copper(II) ions.

Materials and Methods

1. Improved synthesis of NBHB and DBHB

1.1. NBHB: In contrast to the earlier reported low yielding melting procedure (Ortlepp et al. 2007) we now describe an improved synthesis of NBHB. Methyl-[2-hydroximino-3-(4-hydroxyphenyl)]-propionate (4.18 g, 0.02 mol) was triturated with tyramine (6.03 g, 0.044 mol). This mixture was transferred into a small wide-mouth flask and DMF (10 g) was added. The open flask was heated in an oil bath up to 100°C. The resulting amber syrup was magnetically stirred at 135 – 145 °C for 20 minutes and then cooled to room temperature. After addition of water (20 ml) and ethyl acetate (50 ml) the mixture was stirred until nearly all has been dispensed and only small amounts of insoluble polymeric material remained. The liquid was transferred to a separation funnel using additional ethyl acetate (200 ml). The organic layer was washed with water and this phase was extracted exhaustively with ethyl acetate. The combined organic phase was washed successively with 1% HCl (rejected) and 1% aqueous sodium carbonate solution (rejected). The finally remaining ethyl acetate extract was worked up as usual. The after evaporation remaining brown syrup (7 g) was diluted with ethyl acetate (5 ml) and dichloromethane was added drop by drop until turbidness. This mixture was

fractionated on a silica gel column (40 x 5 cm, silica gel 0.064 – 0.2) with dichloromethane/ethyl acetate (1400 + 600) to give after crystallization of the evaporated residue 4.8 g (76.3%) of NBHB as colourless crystals, melting point 178 – 179°C.

1.2. DBHB: NBHB (9.43 g, 0.03 mol) was dissolved in DMF (30 ml) and diluted with dichloromethane (200 ml). After cooling on crashed ice a solution of bromine (150 ml 1M-Br_2 in dichloromethane) was added during 15 minutes under stirring an cooling away from light. Complete bromination was controlled by thin layer chromatography. The excess of bromine was reduced by adding aqueous 10% sodium hydrogen sulphite solution until the brown colour was converted to a pale yellow. The water phase was separated and extracted exhaustively with ethyl acetate. Both organic phases were separately washed with water, then combined, dried over anhydrous sodium sulphate, filtered and concentrated under vacuum. Addition of dichloromethane to the residue resulted in crystallization of 8.5 g pure DBHB. Column chromatography of the mother liquor on silica gel with dichloromethane/ethyl acetate/methanol (1000+100+10) followed by crystallization gave additional 7.7 g of pure DBHB (overall yield 85.7%), melting point 155 – 158°C. $C_{17}H_{14}Br_4N_2O_4$ (629.92): C calcd. 32.41, found 32.59, H calcd. 2.24, found 2.31, N calcd. 4.45, found 4.40. This and the following elementary analyses were carried out using a Perkin-Elmer PE 2400 CHN Elemental Analyzer (Perkin-Elmer Instruments GmbH, Rodgau-Jügesheim, Germany). The analytically pure compound was crystallized for x-ray analysis from hot ethyl acetate by slowly cooling down to room temperature. Crystals were separated, washed with cold ethyl acetate and dried in vacuum at room temperature.

2. Inhibition of phenoloxidase from the blue mussel *Mytilus edulis*: Phenoloxidase activity was measured spectrophotometrically as described by Hellio et al. (2000a): the purified enzyme was incubated at 25°C with 10 mM L-dopa or catechol in 50 mM phosphate buffer of pH 6.8. Phenoloxidase activity was determined by monitoring the increase of absorbance at a wavelength of 475 nm. One unit enzyme activity was defined as the amount of enzyme that catalyzes the formation of 1 µmol dopachrome per minute under the described experimental conditions. Enzyme inhibitors such as DBHB were added to the assay at concentrations up to 50 µg/ml. In addition, the biocide TBTO (10 µg/ml) was used as a positive standard (Hellio et al., 2000a). Aliquots of pure enzyme were incubated for 2 hours with DBHB or other compounds tested as inhibitors, then the enzyme activity was recorded with L-dopa or catechol (10 mM) as substrates. All assays were run in triplicate.

3. Measurement of copper(II)-complex formation of DBHB in solution: DBHB and $CuSO_4$ were dissolved in methanol (Merck p.a.) and added to a 1 cm-cuvette resulting in final concentrations of each 333 µmol DBHB with increasing concentrations of $CuSO_4$ (167, 333, 555, 1111, 1667, and 3333 µmol per ml. The molar ratios between DBHB and $CuSO_4$ were thus 2:1, 1:1.7, 1:3.3, 1:5, and 1:10. Assays were measured photometrically in a cuvette with a thickness of 1 cm in a Perkin Elmer Lambda 25 UV/VIS spectrometer connected with the computer software Perkin Elmer UV winlab 5.1.3.0626. Each sample was measured against methanol containing the same molar concentration of $CuSO_4$ as present in the assay.

4. Neutral copper precipitate of DBHB: DBHB (630 mg, 1 mmol) was dissolved in methanol (20 ml) and copper acetate (182 mg, 1 mmol) in water (20 ml) was added. After addition of excess sodium acetate solution in water the pH was adjusted to 9

and the brown precipitate was removed by suction, washed with water and dried in vacuum at 100°C. The resulting cocoa like powder could be identified as a neutral copper complex where one Cu^{2+} is bound to two deprotonated DBHB molecules. $C_{34}H_{26}Br_8CuN_4O_8$ (1321.37): C calcd. 30.90, found 30.72, H calcd. 1.98, found 2.02, N calcd. 4.24, found 4.13.

5. Selective bastadin precipitation and recovery from a crude extract of the sponge *Ianthella basta*: To an aliquot of a crude methanolic extract of the sponge *I. basta* a surplus of $CuSO_4$ solution in methanol was added. By addition of sodium carbonate the pH of the solution was titrated to pH 11. The formed brown precipitate was recovered by centrifuging (1,000 g) whereas the supernatant was rejected. The pellet was washed twice with sodium carbonate solution and with water followed by addition of 10 ml of diluted HCl. The acidic aqueous phase was partitioned three times against 10 ml ethyl acetate followed by evaporation of the ethyl acetate soluble part using a rotary evaporator. The residue was dissolved in 2 ml methanol, injected into a HPLC machine and analyzed fro bastadin congeners as described previously (Ortlepp et al., 2007).

6. Crystallization of the DBHB complex with copper(II) chloride [Di-μ-chloro-bis(6,6'-dibromohemibastadin-1)(dichloro)bis(dimethylformamido)dicopper(II)]: DBHB (630 mg, 1 mmol) was dissolved in 2-propanol (3 ml). The colourless solution was combined with the light green solution of anhydrous $CuCl_2$ (134 mg, 1 mmol) in 2-propanol (5 ml). The colour of the mixture turned to an intensive dark green. Precipitation of an intensive green powder was completed by cooling over night in a refrigerator. After separation with a suction filter the precipitate was washed with cold 2-propanol and dried in vacuum. Yield 750 mg (98%). This microrystalllinic powder,

however, was not suitable for x-ray analysis. It was nearly insoluble in all common solvents except DMF. Sufficient crystallisation was achieved by slowly dropping dichloromethane into a DMF-solution of the precipitate at room temperature. The light green crystals were separated, washed with dichloromethane and dried in vacuum at 100°C. They were insoluble in water or in dichloromethane but more or less soluble in methanol, ethanol and 2-propanol. Elemental analysis showed DMF and dichloromethane as constituents: [1 DBHB x 1 $CuCl_2$ x 1 DMF x 1 CH_2Cl_2], $C_{21}H_{23}Br_4Cl_4CuN_3O_5$ (922.4): C calcd. 27.34, found 27.30; H calcd. 2.51, found 2.48; N calcd. 4.56, found 4.47. If a solution of this compound in methanol is treated with an excess of aqueous sodium carbonate solution a brown precipitate is formed which was identical with the neutral copper precipitate of DBHB. Successful X-ray-analysis of the complex of DBHB with $CuCl_2$/DMF/dichloromethane could only be achieved with those crystals, which only were carefully dried at room temperature. This material contains more than 1 equivalent of the latter solvent (see below: X-ray crystallographic study). However, if the drying procedure is performed at higher temperature, the required crystalline structure of the material is lost.

7. X-ray Crystallographic Study: Crystal Structure Determinations of compounds $C_{17}H_{14}Br_4N_2O_4$ (DBHB) and ($C_{40}H_{40}Br_8Cl_4Cu_2N_6O_{10} \cdot 4CH_2Cl_2$ ($(DBHB(DMF)CuCl_2)_2 \cdot 4CH_2Cl_2$): Crystals suitable for X-ray study were selected by means of a polarisation microscope and investigated on a STOE Imaging Plate Diffraction System using graphite monochromatized MoKα radiation (λ = 0.71073 Å). To avoid loss of CH_2Cl_2 and deterioration, crystals of the copper compound had to be enclosed in thin walled glass capillaries and the study had to be performed at 173 K. Unit cell parameters were determined by least-squares refinements on the positions of 6074 and 8000 reflections in the range 1.95° < θ < 25.85° and 6.0° < θ < 20.75°, respectively. Space

group type No. 14 was uniquely determined in the case of DBHB. For crystals of the copper compound systematic extinctions were consistent with space group types *Cc* and *C*2/*c*. In accordance with E-statistics significantly better results were observed with a disordered structural model in the centrosymmetric type *C*2/*c*. Corrections for Lorentz and polarization effects and multi-scan absorption corrections were applied for both compounds. The structures were solved by direct methods (Sheldrick, 1990) and subsequent ΔF-syntheses. Approximate positions of all the hydrogen atoms of DBHB and of the dinuclear copper complex were found in different stages of refinements by full-matrix least-squares calculations on F^2 (Sheldrick, 1997). The hydrogen atom positions of the non-coordinated CH_2Cl_2 molecules in the copper compound needed to be calculated. Refinement suffered from the high mobility of these solvent molecules and appropriate distance and displacement parameter restraints and constraints had to be applied to achieve convergence. Anisotropic displacement parameters were refined for all non-hydrogen atoms. For the H atoms at N2, O1 and O3 of $C_{17}H_{14}Br_4N_2O_4$ positional and isotropic displacement parameters were refined. With idealized bonds lengths and angles assumed for all the other OH and NH groups and for all the CH_3, CH_2, and CH groups of both compounds, the riding model was applied for the corresponding H atoms. In addition, the H atoms of the OH groups were given allowance for rotation around the neighbouring O-C axis, and the H atoms of the CH_3 groups were allowed to move collectively around the neighbouring C–C axis. An isotropic displacement parameter was refined for the H atom at N2 of the copper complex. The isotropic displacement parameters of the H atoms not explicitly mentioned here were constrained to 120% of the equivalent isotropic displacement parameters of the parent O, N and C atoms for the NH, CH and CH_2 groups and equal to 150% for the OH and the CH_3 groups. CCDC-782628 ($C_{17}H_{14}Br_4N_2O_4$) and CCDC-782629 ($C_{40}H_{40}Br_8Cl_4Cu_2N_6O_{10} \cdot 4CH_2Cl_2$) contain the

supplementary crystallographic data (excluding structure factors) for this paper. These data can be obtained free of charge from The Cambridge Crystallographic Data Centre *via* www.ccdc.cam.ac.uk/data_request/cif.

Discussion

DBHB, NBHB and 2,3-BMO proved to be strong inhibitors of blue mussel phenoloxidase (**Fig. 1**). The IC_{50} value of the most active compound DBHB (0.84 µM) compares favourably with those of other reported marine-derived blue mussel phenoloxidase inhibitors such as the meroditerpenoids (3aS,7aR)-1,2,3,3a,7,7a-hexahydro-5-(2-hydroxy-2-methylpropyl)-6-((R)-6-methoxy-2,8-dimethyl-2H-chromen-2-yl)-3a,7a-dimethylinden-4-one (IC_{50}: 2.3 µM) or (1Z)-1-((5aR,8aS)-2,3,5,5a,6,7,8,8a-octahydro-2,2,5a,8a-tetramethylindeno[4,5-b]furan-4-ylidene)propan-2-one (IC_{50}: 4.0 µM). Both compounds were isolated previously from the brown alga *Cystoseira baccata* (Mokrini et al. 2008).

Comparison of the structure activity relations of the compounds tested in this study unequivocally proves the importance of the α-oxo-oxime moiety that is the uniting structural feature and the pharmacophore of compounds DBHB, NBHB and or 2,3-BMO but is lacking in the nearly inactive active compound TT. Presence of the phenolic rings and of the bromine substituents as observed for compounds DBHB and NBHB enhances the enzyme inhibitory activity in comparison to compound 2,3-BMO by factors of 3.6 (2,3-BMO vs. NBHB) and 10.3 (2,3-BMO vs. DBHB) whereas replacement of the α-oxo-oxime group by an α-oxo-amino group as present in TT causes a dramatic drop in activity (by a factor of > 34 compared to the closest structural analogue NBHB, **Fig 1**). Interestingly, the differential degree of inhibition of

blue mussel phenoloxidase by DBHB, NBHB and TT is paralleled by their antifouling activity against larvae of the barnacle *Amphibalanus improvisus* that was reported earlier (Ortlepp et al., 2007). In a settling bioassay DBHB proved to be the most active compound with an IC_{50} value between 1 – 10 µM followed by NBHB (IC_{50}: 10 – 100 µM) whereas TT (4) was inactive up to 100 µM (2,3-BMO had not been tested in the original experiment with *B. improvisus*) (Ortlepp et al., 2007) thus indicating that the *in vitro* inhibition of phenoloxidase as documented in this study is apparently also of relevance under *in vivo* conditions. Hemibastadin derivatives as analyzed in this study are not the only sponge-derived compounds featuring an α-oxo-oxime group known from nature. Besides other compounds belonging to the bastadin family we were previously able to show that for example aplysamine-2 isolated from the sponge *Pseudoceratina purpurea* and psammaplin A obtained from the sponge *Aplysinella rhax* likewise suppress settling of barnacle larvae at concentrations similar to those of bastadin derivatives or of DBHB (Ortlepp et al., 2007).

No enzyme inhibitory studies were conducted for the latter compounds. However, based on the obvious structural similarities with DBHB, especially with regard to the important α-oxo-oxime group it is very probable that these as well as other natural products featuring this pharmacophoric group (see e.g. Blunt et al., 2009 and previous reviews in this series) will likewise inhibit blue mussel phenoloxidase.

Inhibition of blue mussel phenoloxidase by DBHB, NBHB and 2,3-BMO analyzed in this study is reflected by their ability to complex copper(II) ions (e.g. as shown for DBHB in **Fig. 5**) whereas compound TT failed to do this. Complexation of copper(II) ions was also demonstrated in this study for a naturally occurring mixture of bastadin derivatives as present in a crude extract of the sponge *I. basta*. Comparative X-ray

structure determinations of DBHB and the dinuclear copper(II) complex $(DBHB(DMF)CuCl_2)_2 \cdot 4CH_2Cl_2$ as well as the comparison with structurally related complexes characterize DBHB as N,O-bidentate chelating ligand with strong binding potential for copper(II).

In conclusion: This study demonstrates for the first time the strong inhibition of blue mussel phenoloxidase by DBHB and by structurally related compounds at submicromolar to low micromolar concentrations. Additional experimental evidence obtained earlier with barnacle larvae (Ortlepp et al., 2007) furthermore indicates that inhibition of the target molecule phenoloxidase extends also to the *in vivo* level. We provide evidence for the α-oxo-oxime group as the decisive pharmacophore of the studied molecules that is responsible for the complexation of copper(II) ions as shown by X-ray analysis of a copper(II) complex of DBHB. The data presented finally suggest that the documented strong inhibition of blue mussel phenoloxidase is mechanistically due to complexation of copper(II) ions that are present within the catalytical centre of the enzyme.

Acknowledgement: Financial support of the BMBF to Peter Proksch under the project *BiotecMarin* is gratefully acknowledged. We thank the Industrieclub Düsseldorf e.V. for financial support of Mirko Bayer and Mrs Eleonore Hammes for technical assistance during the X-ray diffraction experiments.

Literature

Aladaileh S, Rodney P, Nair SV, Raftos DA (2007). Caharcterization of phenoloxidase activity in Sydney rock oysters (*Saccostrea glomerata*). Comparative Biochemistry and Physiology, Part B. 148: 470-480

Asokan R, Arumugam M, Mullainadhan P (1997). Activation of prophenoloxidase in the plasma and haemocytes of the marine mussel *Perna viridis* Linnaeus. Developmental and Comparative Immunology. 21: 1-12

Blunt J.W., Copp B.R., Hu W.-P.H., Munro M.H.G., Northcote P.T., Prinsep M.R. (2009). Marine natural products. Nat. Prod. Rep. 26: 170 - 244

Chen JS, Wei C, Rolle RS, Otwell WS, Balaban MO, Marshall MR (1991). Inhibitory Effect of Kojic Acid on Some Plant and Crustacean Polyphenol Oxidases. J. Agric. Food Chem. 39: 1396-1401

Cheung PJ, Ruggieri GD, Nigrelli RF (1977). A New Method for Obtaining Barnacle Cement in the Liquid State for Polymerization Studies. Marine Biology. 43: 157-163

Cima, F., Ballarin, L., 2000. Tributyltin induces cytoskeletal alterations in the colonial ascidian *Botryllus schlosseri* phagocytes via interaction with calmodulin. Aquat. Toxicol. 48: 419–429.

Cima, F., Ballarin, L., Bressa, G., Burighel, P., 1998a. Cytoskeleton alterations of tributyltin (TBT), in lunicante phagocytes. Ecotoxicol. Environ. Saf. 40, 160–165.

Cima, F., Spinazzi, R., Ballarin, L., 1998b. Possible tributyltin–calmodulin interaction in morphofunctional alterationsof ascidian phagocytes. Fresenius Environ. Bull. 7, 396–401.

Clare AS (1996). Signal transduction in barnacle settlement: calcium re-visited. Biofouling. 10: 141-159

Clare AS, Hoeg JT (2008). *Balanus amphitrite* or *Amphibalanus amphitrite*? A note on barnacle nomenclature. Biofouling. 24: 55-57

Decker H, Dillinger R, Tuczek F (2000). Wie funktioniert die Tyrosinase? Neue Einblicke aus Modellchemie und Strukturbiologie. Angew. Chem. 112: 1656-1660

Hellio C, Bourgougnon N, Le Gal Y (2000). Phenoloxidase (E.C. 1.14.18.1) from *Mytilus edulis* byssus gland: purification, partial characterization and application for screening products with potential antifouling activities. Biofouling. 16: 235-244

Fusetani N (2004). Biofouling and antifouling. Nat Prod. Rep. 21: 94-104

Hellio C, Bado-Nilles A, Gagnaire B, Renault T, Thomas-Guyon H (2007). Demonstration of a true phenoloxidase activity and activation of a ProPO cascade in Pacific Oyster, *Crassostrea gigas* (Thunberg) in vitro. Fish & Shellfish Immunology. 22: 433-440

Hellio C, Maréchal JP, Da Gama BAP, Pereira R, Clare AS (2009) Natural marine products with antifouling activities In: Advances in marine antifouling coatings and technologies. Woodshead, Cambridge, pp 572–622

Hellio C, Yebra DM (2009). Legislation affecting antifouling products. In: Advances. In marine antifouling coatings and technologies. Woodshead, Cambridge, pp 240-260

Kamino K (2001). Novel barnacle underwater adhesive protein is a charged amino acid-rich protein constituted by a Cys-rich repetitive sequence. Biochem J. 356: 503-507

Kapoor P, Pathak A, Kapoor R, Venugopalan P, Corbella M, Rodríguez M, Robles J, Llobet A (2002). Structural, Electronic, and Magnetic Consequences of O-Carbonyl vs O-Alkoxy Ester Coordination in New Dicopper Complexes Containing the $Cu_2(\mu\text{-}Cl)_2$ Core. Inorg. Chem. 41: 6153-6160

Kapoor P, Pathak A, Prabhjot K, Venugopalan P, Kapoor R, (2004). Steric control of coordination: Unusual coordination mode of dimethylpyridine-2,6-dicarboxylate in a new dinuclear copper(II) complex [(dmpc)(Cl)(μ-Cl)Cu_2(μ-Cl)(Cl)(dmpc)] and reversal of the coordination mode in [Cu(dmpc) $(H_2O)_3$] $(ClO_4)_2$. Trans. Met. Chem. 29: 251-258.

Kim D, Park J, Kim J, Han C, Yoon J, Kim N, Seo J, Lee C (2006). Flavonoids as Mushroom Tyrosinase Inhibitors: A Fluorescence Quenching Study. J. Agric. Food Chem. 54: 935-941

Kim YJ, Uyama H (2005). Tyrosinase inhibitors from natural and synthetic sources: structure, inhibition mechanism and perspective for the future. Cell. Mol. Life Sci. 62: 1707-1723

Kubo I, Kinst-Hori I, Chaudhuri SW, Kubo Y, Sánchez Y, Ogura T (2000). Flavonols from *Heterotheca inuloides*: Tyrosinase Inhibitory Activity and Structural Criteria. Bioorganic and Medicinal Chemistry. 8: 1749-1755

Lau M (1991). Tributyltin antifouling: a treat to the Hong Kong marine environment. Arch Environ Contam Toxicol. 20: 299-304

Liu D, Maguire R, Lau Y, Pacepavicius G, Okamura H, Aoyama I (1997). Transformation of the new antifouling compound Irgarol 1051 by Phanerochaete chrysosporium. Water Res. 31: 2363-2369

Marechal JP, Hellio C (2009). Challenges for the development of new non-toxic antifouling solutions. Int J Mol Sci. 10: 4623-37

Mokrini R, Mesaoud MB, Daoudi M, Hellio C, Maréchal JP, El Hattab M, Ortalo-Magné A, Piovetti L, Culioli G (2008). Meroditerpenoids and Derivatives from the Brown Alga Cystoseira baccata and Their Antifouling Properties. J Nat Prod. 71: 1806-1811

Nagasawa T, Utagawa T, Goto J, Kim CJ, Tani Y, Kumagai H, Yamada H (1981). Syntheses of L-Tyrosine-Related Amino Acids by Tyrosine Phenol-lyase of Citrobacter intermedius. Eur J Biochem. 117: 33-40

Olivares C, García-Borrón J, Solano F (2002). Identification of Active Site Residues Involved in Metal Cofactor Binding and Stereospecific Substrate Recognition in Mammalian Tyrosinase. Implications of the Catalytic Cycle. Biochemistry. 41: 679-686

Ortlepp S, Sjögren M, Dahlström M, Weber H, Ebel R, Edrada RA, Thoms C, Schupp P, Bohlin L, Proksch P (2007). Antifouling Activity of Bromotyrosine-Derived Sponge Metabolites and Synthetic Analogues. Mar Biotechnol. 9: 776-785

Pereira M, Ankjaergaard C (2009). Legislation affecting antifouling products. In: Advances. In marine antifouling coatings and technologies. Woodshead, Cambridge, pp 240-260

Rittschof D, Maki J, Mitchell R, Costlow JD (1986). Ion and neuropharmacological studies of barnacle settlement. Neth J Sea Res. 20: 269-275

Sheldrick GM (1990). SHELXS97. Program for the Solution of Crystal Structures, University of Göttingen, Germany

Sheldrick GM (1997). SHELXL97. Program for the Refinement of Crystal Structures, University of Göttingen, Germany

Sommerer SO, Westcott BL, Jircitano AJ, Abboud KA (1995). The synthesis and structure of two novel metal-di-2-pyridyl ketone oxime dimers. Inorganica Chimica Acta, 238: 149-153

Suci PA, Geesey GG (2000). Influence of Sodium Periodate and Tyrosinase on Binding of Alginate and Adlayers of *Mytilus edulis* Foot Protein 1. Journal of Colloid and Interface Science. 230: 340-348

Tsoukatou M, Hellio C, Vagias C, Harvala C, Roussis V (2002). Chemical defense and antifouling activity of three Mediterranean sponges of the genus Ircinia. Z Naturforsch 57:161–171

Tsoukatou M, Maréchal JP, Hellio C, Novaković I, Tufegdzic S, Sladić D, Gašić MJ, Clare AS, Vagias C, Roussis V (2007) Evaluation of the activity of the sponge metabolites avarol and avarone and their synthetic derivatives against fouling micro- and macroorganisms. Molecules 12:1022–1034

Tujula N, Radford J, Nair SV, Raftor DA (2001). Effects of tributyltin and other metals on the phenoloxidase activation system of the tunicate, *Styela plicata*. Aquatic toxicology. 55: 191-201

Voulvoulis N, Scrimshaw M, Lester J (1999). Alternative antifouling biocides. Appl Organometal Chem. 13: 135-145

Wahl N (1989) Marine epibiosis. 1 Fouling and antifouling - some basic aspects. Mar Ecol Prog Ser 58, 175–189

Yamamoto H, Satuito CG, Yamazaki M, Natoyama K, Tachibana A, Fusetani N (1998). Neurotransmitter blockers as antifoulants against planktonic larvae of the barnacle Balanus amphitrite and the mussel *Mytilus galloprovincialis*. Biofouling. 13: 69-82

Yebra DM, Kiil S, Dam-Johansen K (2004) Antifouling technology: past, present and future steps towards efficient and environmentally friendly antifouling coatings. Progr Org Coating 50:75–104

Zentz F, Hellio C, Valla A, De La Broise D, Bremer G, Labia R (2002). Antifouling Activities of N-Substituated Imides: Antimicrobial Activities and Inhibition of *Mytilus edulis* Phenoloxidase. Mar Biotechnol. 4: 431-430

Figures

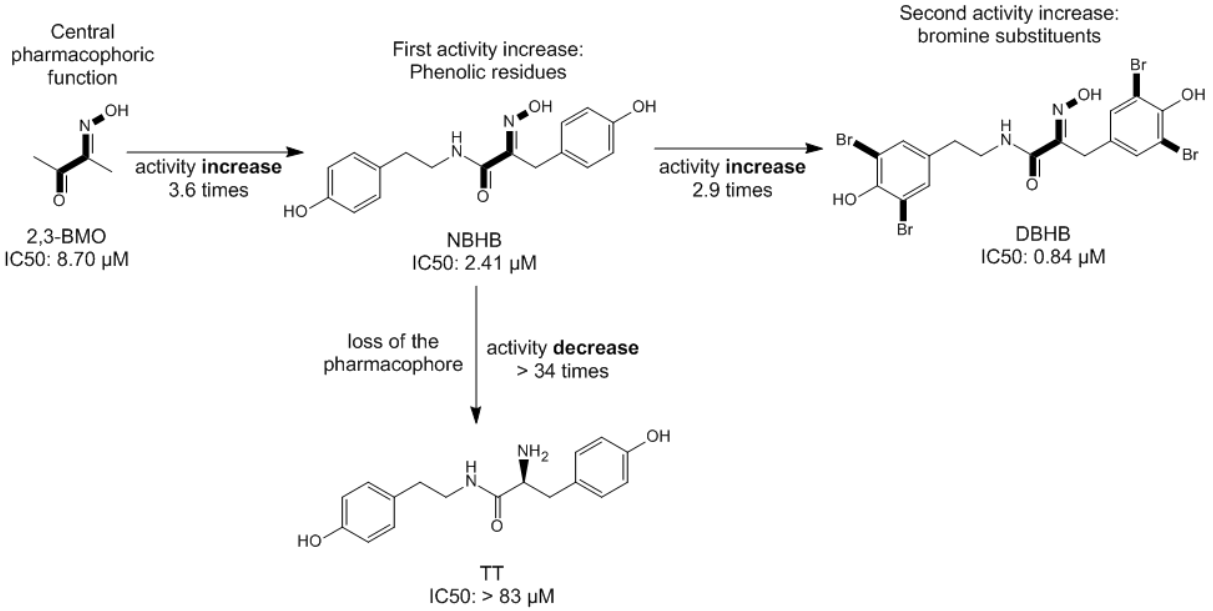

Fig. 1: Inhibition of blue mussel phenoloxidase by 2,3-BMO, NBHB, DBHB and TT as indicated by the IC_{50} values of the respective compounds obtained from *in vitro* experiments.

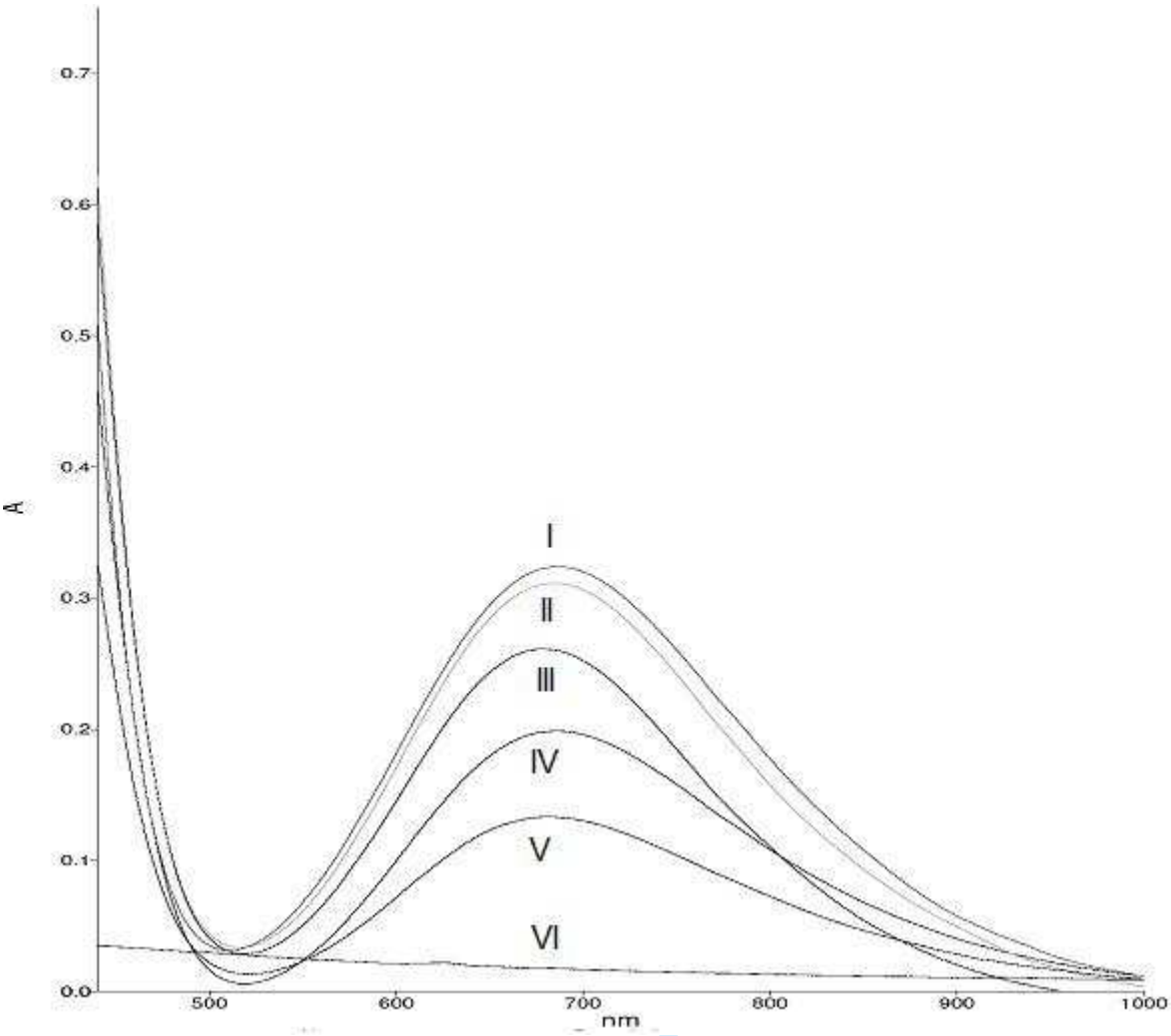

Fig. 2: Part of the absorption spectra of DBHB (333 µmol) with various concentrations of $CuSO_4$ in methanolic solution: (I) 3333 µmol $CuSO_4$/ml; (II) 1667 µmol $CuSO_4$/ml; (III) 1111 µmol $CuSO_4$/ml; (IV) 555 µmol $CuSO_4$/ml; (V) 167 µmol $CuSO_4$/ml; (VI) 0 µmol $CuSO_4$/ml

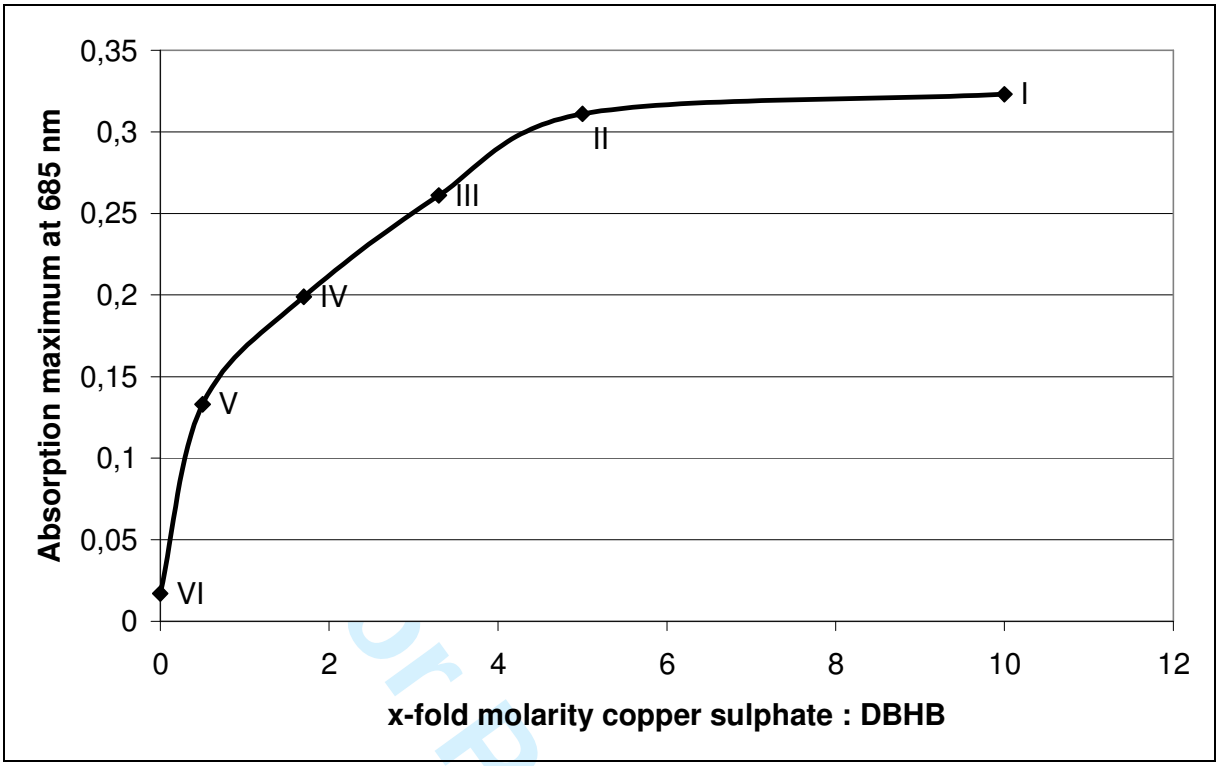

Fig. 3: Influence of the different molar ratios of DBHB and $CuSO_4$ on the absorption maxima at 685 nm: (I) 1:10; (II) 1:5; (III) 1:3.3; (IV) 1:1.7; (V) 1:0.5; (VI) only DBHB without Cu(II)SO_4

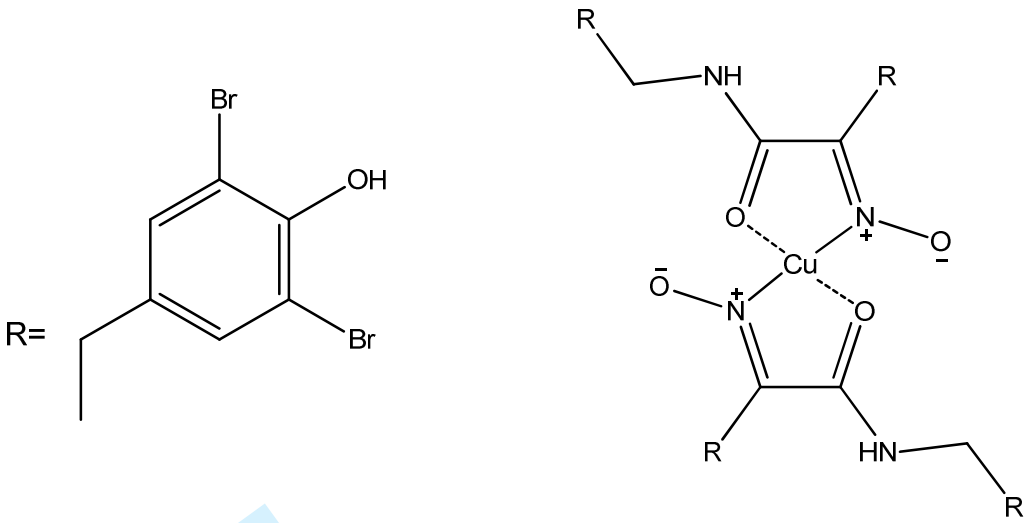

Fig. 4: Proposed structure of the neutral copper(II)-precipitate of DBHB

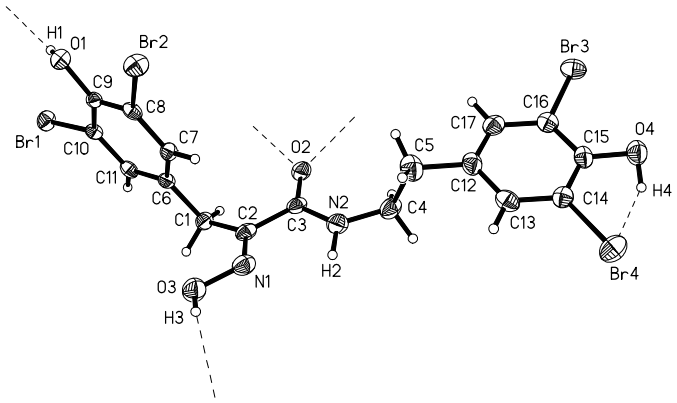

(a) DBHB

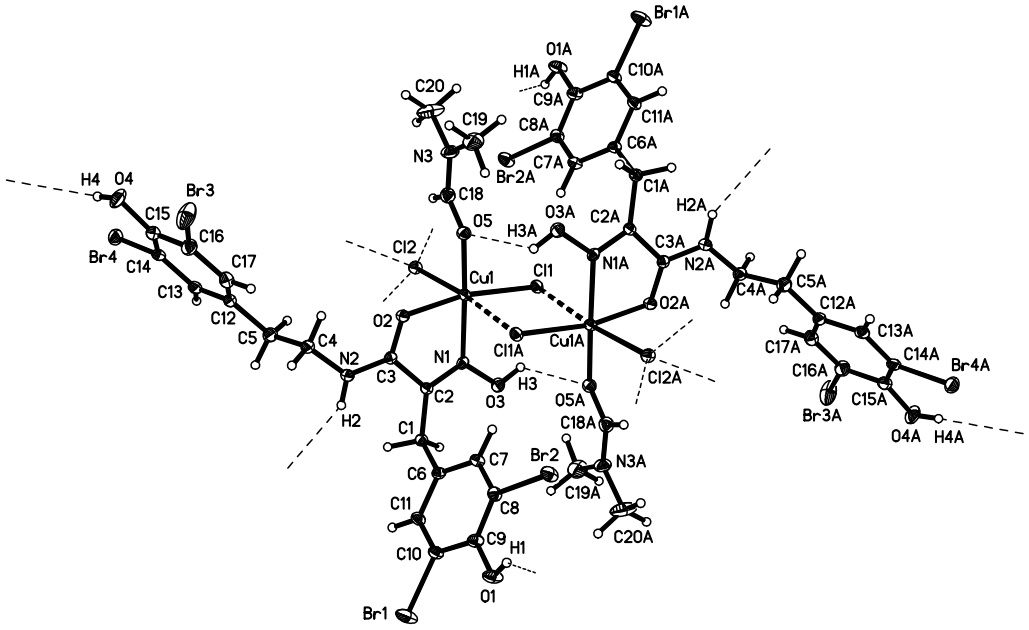

(b) $(DBHB(DMF)CuCl_2)_2 \cdot 4CH_2Cl_2)$

Fig. 5: Molecular structure of DBHB in the crystal (30 % probability ellipsoids) (**a**) and structure of the dinuclear complex di-μ-chloro-bis(6,6'-dibromohemibastadin-1)(dichloro)bis(dimethylformamide)dicopper(II) in its crystalline tetrakis(dichoromethane) solvate (25 % probability ellipsoids) (**b**). The directions of supramolecular association *via* hydrogen bonding are indicated by dashed lines.

Table 1 Selected bond lengths (in Å) and angles (in °) for DBHB (**1**) and $(DBHB(DMF)CuCl_2)_2 \cdot 4CH_2Cl_2$ (**2**)

	1	**2**		**1**	**2**
Br1–C10	1.908(5)	1.892(6)	N3–C19		1.454(8)
Br2–C8	1.898(5)	1.919(5)	N3–C20		1.448(9)
Br3–C16	1.908(5)	1.903(6)	C1–C2	1.499(7)	1.497(7)
Br4–C14	1.891(5)	1.906(6)	C1–C6	1.517(7)	1.530(7)
Cu1–Cl1		2.2920(15)	C2–C3	1.504(7)	1.511(7)
Cu1–Cl2		2.6420(13)	C4–C5	1.500(8))	1.526(8)
Cu1–Cl1*A*		2.9384(14)	C5–C12	1.530(8)	1.517(8)
Cu1–O2		2.000(4)	C6–C7	1.397(7)	1.390(7)
Cu1–O5		1.962(4)	C6–C11	1.382(6)	1.388(8)
Cu1–N1		1.999(4)	C7–C8	1.389(6)	1.388(8)
O1–C9	1.350(6)	1.356(7)	C8–C9	1.396(7)	1.367(9)
O2–C3	1.245(5)	1.259(6)	C9–C10	1.390(7)	1.406(8)
O3–N1	1.401(6)	1.370(5)	C10–C11	1.385(7)	1.391(8)
O4–C15	1.359(6)	1.361(7)	C12–C13	1.412(8)	1.394(8)
O5–C18		1.248(7)	C12–C17	1.412(8)	1.389(8)
N1–C2	1.280(6)	1.283(7)	C13–C14	1.379(8)	1.379(8)
N2–C3	1.336(7)	1.307(7)	C14–C15	1.391(7)	1.398(8)
N2–C4	1.459(7)	1.468(7)	C15–C16	1.381(7)	1.412(9)
N3–C18		1.316(8)	C16–C17	1.388(8)	1.368(9)

	2		**1**	**2**
Cl1–Cu1–Cl2	96.82(5)	O3–N1–C2	112.3(5)	116.3(4)
Cl1–Cu1–Cl1*A*	87.14(5)	C6–C1–C2	114.9(4)	112.7(4)
Cl1–Cu1–O2	168.91(11)	N1–C2–C1	125.5(5)	125.4(5
Cl1–Cu1–O5	97.41(12)	N1–C2–C3	115.0(5)	109.0(5)
Cl1–Cu1–N1	90.79(13)	C1–C2–C3	119.5(4)	125.5(5)
Cl2–Cu1–Cl1*A*	174.85(5)	O2–C3–N2	121.8(5)	122.9(5)
Cl2–Cu1–O2	87.87(10)	O2–C3–C2	121.6(5)	118.5(5)
Cl2–Cu1–O5	96.82(11)	N2–C3–C2	116.5(4)	118.6(5)
Cl2–Cu1–N1	94.02(12)	C3–N2–C4	124.7(5)	122.3(5)
Cl1*A*–Cu1–O2	87.65(11)	N2–C4–C5	116.1(3)	110.4(4)
Cl1*A*–Cu1–O5	85.89(11)	C4–C5–C12	110.2(5)	114.7(5)
Cl1*A*–Cu1–N1	82.59(12)	O5–C18–N3		124.8(5)
O5–Cu1–O2	91.98(16)	C18–N3–C19		123.0(6)
O5–Cu1–N1	165.52(17)	C18–N3–C20		120.6(6)
O2–Cu1–N1	78.83(16)	C19–N3–C20		116.3(6)
Cu1-O2-C3	113.8(3)			
Cu1-N1-C2	118.9(3)			

Symmetry code: A 1.5–x, 0.5–y, 2–z

Table 2 The hydrogen bond geometries (in Å and °) for DBHB (**1**) and $(DBHB(DMF)CuCl_2)_2 \cdot 4CH_2Cl_2$ (**2**)

D–H···A	D–H	H···A	angle	D···A
Compound **1**				
O1–H1···O2*A*	0.83(5)	1.92(5)	148(5)	2.663(5)
O3–H3···O2 *B*	0.80(6)	2.29(6)	154(6)	3.031(6)
O4–H4···Br4	0.82	2.60	120.5	3.099(4)
Compound **2**				
N2–H2···Cl2*C*	0.88	2.42	152.4	3.228(5)
O1–H1···Cl2*D*	0.84	2.35	146.2	3.080(4)
O3–H3···O5*E*	0.84	2.58	112.3	3.003(5)
O4–H4···Cl2*F*	0.84	2.48	137.0	3.151(4)

Symmetry codes: A 1–x, 1–y, 1–z; *B* 1–x, y–0.5, 0.5–z; *C* x, 1–y, z–0.5; *D* 1.5–x, y–0.5, 1.5–z; *E* 1.5–x, 0.5–y, 2–z;*F* 1–x, y, 1.5–z

Table 3: Summary of crystal data, details of intensity measurements and structure refinements of DBHB and $((DBHB(DMF)CuCl_2)_2 \cdot 4CH_2Cl_2)$.

	$C_{17}H_{14}Br_4N_2O_4$	$C_{40}H_{42}Br_8Cl_4Cu_2N_6O_{10} \cdot 4CH_2Cl_2$
Empirical formula	$C_{17}H_{14}Br_4N_2O_4$	$C_{44}H_{50}Br_8Cl_{12}Cu_2N_6O_{10}$
M_r	629.90	2014.60
Crystal system	monoclinic	monoclinic
Space group	$P2_1/c$	$C2/c$
Z	4	4
Temperature [K]	291(2)	173(2)
Unit cell parameters		
a [Å]	8.8333(5)	33.0662(19)
b [Å]	13.9719(10)	14.7836(11)
c [Å]	16.2404(13))	13.9389(7)
β [°]	100.255(8)	100.841(6)
Volume [Å^3]	1999.7(2)	6692.3(7)
$D_{calcd.}$	2.092	2.000
Absorption coefficient	8.076	5.946
F(000)	1208	3912
Crystal size [mm^3]	0.23 x 0.22 x 0.09	0.28 x 0.25 x 0.03
Crystal colour	colourless	green
Diffractometer type	Stoe-IPDS	Stoe-IPDS
Scan mode	φ	φ
θ range for data collection	1.92-25.00	2.04-25.00
Limiting indices	-10< h < 10	-39 < h < 39
	-16< k < 16	-17 < k < 17
	-19 < l < 19	-16 < l < 15
Reflections collected	18311	43969
Reflections unique	3502	5808
Reflections observed	2391	4235
Criterion for observation	$I > 2\sigma(I)$	$I > 2\sigma(I)$
Completeness	0.994	0.983
Refined Parameters	256	392
R_1[a], observed	0.035	0.045
wR_2[b], all data	0.072	0.112
Goodness-of-Fit, S[c]	1.01	1.13
Largest diff. peak/hole	0.63/-0.34	2.29/-1.10
CCDC-identifier	782628	782629

[a] $R_1 = || F_o|-|F_c||/|F_o|$; [b] $wR_2 = [w(F_o^2-F_c^2)^2/w(F_o^2)^2]^{1/2}]$, where $w = 1/[\sigma^2(F_o^2)+(aP^2)]$ and $P = (F_o^2+2F_c^2)/3$; [c] $S = [w(F_o^2-F_c^2)^2/(n-p)]^{1/2}$.